

# A General Airgap Field Modulation Theory for Electrical Machines

Ming Cheng, *Fellow, IEEE*, Peng Han, *Student Member, IEEE*  
and Wei Hua, *Senior Member, IEEE*

**Abstract**—This paper proposes a general field modulation theory for electrical machines by introducing magnetomotive force modulation operator to characterize the influence of short-circuited coil, variable reluctance and flux guide to the primitive magnetizing magnetomotive force distribution established by field winding function multiplied by field current along the airgap peripheral. Magnetically anisotropic stator and rotor behave like modulators to produce a spectrum of field harmonics and the armature winding plays the role of a spatial filter to extract effective field harmonics to contribute the corresponding flux linkage and induce the electromotive force. The developed field modulation theory not only unifies the principle analysis of a large variety of electrical machines, including conventional DC machine, induction machine and synchronous machine which are just special cases of the general field modulated machines, thus eliminating the problem of the machine theory fragmentation, but also provides a powerful guidance for inventing new machine topologies.

**Index Terms**—Air gaps, analytical models, electric machines, filter, magnetic fields, modulation, power conversion, spectral analysis, general theory.

## NOMENCLATURE

$\gamma$	Coil span factor of a specific coil
$\varphi$	Mechanical rotor angular position with respect to the stationary stator
$\delta$	Skewing angle
$\varepsilon$	Pole-arc to pole-pitch ratio of simple salient pole
$\theta, \phi$	Mechanical angle along the circumference in stationary reference frame, modulator-fixed reference frame
$\mu_0$	The permeability of vacuum
$\nu$	Generic harmonic order
$\tau^j(\theta, \varphi)$	Turn function of $j$ -th phase winding
$\psi$	Flux linkage
$\omega_r$	Mechanical angular velocity of modulator

$B(\theta, t)$	Airgap flux density distribution function
$\overline{B}_a^\nu, \overline{J}_a^\nu$	Specific magnetic loading, electric loading of $\nu$ -order harmonic of armature side
$B_{a(\text{amp})}^\nu, B_g$	Flux density amplitude of the $\nu$ -order field harmonic component, airgap flux density
$C^S, C^R$	Discontinuous intervals occupied by stator, rotor teeth
$\cos \varphi_a^\nu$	Airgap power factor of $\nu$ -order harmonic specific electromagnetic loading ( $\overline{B}_a^\nu, \overline{J}_a^\nu$ ) of armature side
$d, r_g$	Diameter, radius of airgap
$E$	The set of orders of effective components of the modulated MMF
$e$	Electromotive force (EMF)
$F(\theta, t)$	Primitive magnetomotive force (MMF) distribution function
$F_\nu, \varphi_\nu$	$\nu$ -th MMF harmonic amplitude, phase angle
$g, g^{-1}(\theta)$	Airgap length, inverse airgap function
$I_{a(\text{rms})}^j$	The rms value of the $j$ -th phase armature current
$i^j$	Current flowing in the $j$ -th short-circuited coil
$k_{w\nu}, k_{s\nu}, k_{c\nu}$	Winding factor, skew factor, composition factor of generic harmonic order $\nu$
$L_{stk}$	Stack length
$M[\cdot]$	Modulation operator
MF	Modulation factor
$m$	Phase number
$N_a^j$	Number of turns in series of the $j$ -th phase armature winding
$N_{MB}$	Number of flux guide segment
$N_{SC}$	Number of short-circuited coil group
$N_{ST}, N_{RT}$	Simple salient pole number of stator, rotor
$o, t_d$	Slot opening width, tooth pitch
$p$	Principal pole pair number
$T_{em}$	Electromagnetic torque
$T_{Mf(\omega)f}$	Electromagnetic torque produced by interaction between modulated magnetizing MMF and modulated magnetizing (armature) MMFs
$T_{Mf(\omega)a}$	Electromagnetic torque produced by interaction between modulated armature MMF and modulated magnetizing (armature) MMF
TRV	Torque per rotor volume
$W^j(\theta, \varphi)$	Winding function of $j$ -th phase winding
<b>Subscripts</b>	
$f, a$	Field winding, armature winding
$ST, RT$	Stator tooth, rotor tooth

Manuscript received September 18, 2016; revised December 10, 2016; accepted December 30, 2016. This work was supported in part by the 973 Program of China under Project 2013CB035603, in part by the National Natural Science Foundation of China under Projects 51320105002 and 51137001.

The authors are with the School of Electrical Engineering, Southeast University, Nanjing 210096, China (e-mail: mcheng@seu.edu.cn; hanpeng360001@163.com; huawei1978@seu.edu.cn).

$s, r$  Stator, rotor

## I. INTRODUCTION

**E**LECTRICAL machines are physical devices to accomplish continuous electromechanical energy conversion through magnetic field or electric field coupling. Due to the fact that the energy density of dielectric material is still much lower than that of magnetic material at present, almost all electrical machines adopt magnetic field coupling. Since Jacobi invented the first direct current machine (DCM) in 1834 and Ferraris and Tesla invented the first induction machine (IM) in late 1880s, electromagnetic machine has been a prime source of mechanical/electrical power for the past centuries [1], with the power ranging from several nano-watts to hundreds of mega-watts. Besides the conventional DCM, IM and synchronous machine (SM), a vast variety of other electromagnetic machines have been resurging or emerging to meet various performance requirements, such as the synchronous reluctance machine (SynRM) [2], the permanent magnet brushless (PMBL) machines [3], [4], the vernier machine [5], the brushless doubly-fed induction machine (BDFIM) [6], [7], the brushless doubly-fed reluctance machine (BDFRM) [8], the transverse flux machine (TFM) [9], the switched reluctance machine (SRM) [10], the stator-PM machines with doubly salient structure [11], [12], the permanent magnet vernier (PMV) machine [13], the magnetic gear (MG) [14] and magnetically-g geared machine (MGM) [15-17], the dual-mechanical-port (DMP) machine [18], and so on. Meanwhile, different analytical theories have been developed to analyze the underlying operation principle and electromagnetic performance of these machines, such as the winding function theory [19] and the unified theory of torque production based on the trajectory of the phase flux linkage versus phase current [ $i-\psi$ ] [20], the rotating field theory [21] and cross-field theory [22] for ac machines, well-known two-reaction theory for SM [23], [24], the general theory based on the two-axis primitive machine model [25] and the general theory using equivalent magnetic circuits [26]. Though all these established theories have ever brought great conveniences to analysis and design of conventional machines like DCM, IM, SM, etc., they show weakness in effectively analyzing a large proportion of newly-emerged machines with multi-harmonic and multi-port features, like BDFIM, BDFRM, and stator-PM machines, etc. For example, the general theory developed by Adkins et al. based on the ideal machine model [25] is only valid or accurate for AC machines with sinusoidal current, but not valid for DC machines. The general theory by using equivalent magnetic circuits is valid for the analysis of both AC and DC machines, but it cannot reveal the mechanism of energy conversion across the airgap.

With the unprecedented invasion of new electrical machine structures in the rush to electrification of the world during past decades, the theories and methods for analysis of operation mechanism, performance calculation and design principle, etc., are becoming more and more machine-specific and fragmented. Therefore it becomes a significant and urgent task to construct a

systematic and theoretical explanation and guidance to invent, analyze and design new machine topologies to avoid blindness, contingency and overreliance on empirical knowledge.

The purpose of this paper is to develop a general theory to present the operating principle and torque production mechanism of all electromagnetic machines in a unified way starting from the widely observed field modulation phenomenon. The general theory introduces topological analysis into the standard analysis procedure of all electrical machines, facilitating the solving of topological problems, like the pole/slot combination, winding configuration, skewing, segmentation, etc. It also resurges the design related issues, such as the redefinition of specific electromagnetic loadings and the standardized representation of torque density equations for initial sizing and quantitative comparison. In addition, it can serve as a powerful tool in inventing new topologies as well as the related feasibility evaluation.

## II. FIELD MODULATION THEORY

An electrical machine usually has an airgap, which is a narrow layer of air, sandwiched by the stationary member, stator, and the rotating/moving member, rotor. Both the stator and rotor are made of soft magnetic materials featuring large relative permeance to air. PMs or field windings mounted on stator or rotor are to establish magnetic field whilst armature windings mounted on stator or rotor are to induce electromotive force (EMF) through cutting the magnetic lines.

As an electromechanical energy converter, the electrical machine shows remarkable resemblance to the switching converter, as illustrated in Fig. 1. Corresponding spectrums are also given to show the similarities in frequency domain.

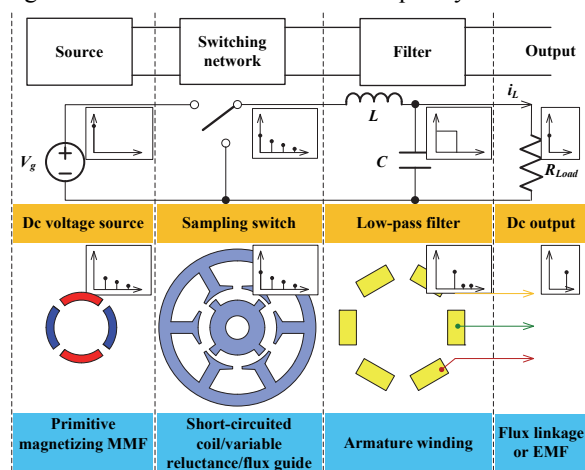


Fig. 1 Analogy between the electrical machine and the switching converter

According to the analogy, an electrical machine is a cascade of three elementary parts, that is, the primitive magnetizing magnetomotive force (MMF) (source), the short-circuited coil/variable reluctance/flux guide (modulator) and the armature winding (filter). The primitive magnetizing MMF establishes an initial MMF distribution with possible spatial harmonics along the physical airgap. The short-circuited coil/variable reluctance/flux guide modulates the initial MMF distribution to produce a spectrum of MMF harmonic

components, for which they are termed as modulators. All the MMF components produce corresponding magnetic field components in the airgap. The armature winding plays the role of a spatial filter selecting effective airgap field harmonics to produce flux linkage or EMF, then feeds the electric load in generating mode or receives the synchronous current to provide mechanical output in motoring mode. The MMF component that can produce effective airgap field harmonic is termed as effective MMF component.

To simplify the establishment of mathematical model, some basic assumptions should be made, as given below:

- PMs are treated as single-phase concentrated windings wrapped around a material with the same permeability as that of the magnet;
- The iron core has infinite magnetic permeance;
- Conductors in each slot are concentrated at the middle point of slot opening;
- Flux lines produced by magnetizing MMF in the airgap is perpendicular to the circumference;
- The flux leakage and the effect of finite axial length are neglected;
- The MMF drop in the iron of machines due to saturation is considered as a constant discount on the airgap MMF.

#### A. Winding Function

Winding layout has a significant influence on the MMF established and EMF induced, and can be fully described by its winding function  $W^j(\theta, \varphi)$  ( $j$ -th phase) obtained from the detailed winding distribution along an equivalent smooth airgap, and

$$W^j(\theta, \varphi) = \tau^j(\theta, \varphi) \frac{\int_0^{2\pi} g^{-1}(\theta) \tau^j(\theta, \varphi) d\theta}{\int_0^{2\pi} g^{-1}(\theta) d\theta} \quad (1)$$

where  $\tau^j(\theta, \varphi)$  is the turn function of  $j$ -th phase,  $\theta$  is the mechanical angle along the circumference in stationary reference frame, and  $\varphi$  is the mechanical rotor angular position with respect to the stationary stator.  $g$  is the airgap length.

The function of the winding function is two-fold: to produce the primitive MMF by multiplying the winding function with the current and to produce flux linkage by integrating the winding function multiplied by the airgap flux density.

The most important features of winding function are the principal pole pair number (PPN)  $p$  and winding factor of each harmonic  $k_{wv}$ . The PPN of a given winding is defined as the pole pair number of the winding function harmonic component that has the largest relative amplitude. With this definition, the  $p$ -pole-pair winding can produce the largest  $p$ -pole-pair MMF component and extract the most  $p$ -pole-pair field harmonic component to produce flux linkage and further EMF.

Expressing the winding function in the form of Fourier series produces a more easy-to-use performance indicator, that is, the winding factor  $k_{wv}$ . Besides short pitch and distribution which have been taken into account by winding factor, the composition between different phases also impacts the MMF and line-to-line EMF, which will be characterized by the composition factor  $k_{cv}$ . In addition, skewing or axial segmentation (discontinuous skewing) changes the relative

placement of airgap field in axial direction, and form a distribution effect [27], [28], which can be characterized by the skew factor  $k_{sv}$  [29]. Taking the three factors into account leads to the concise expression of the MMF as

$$F(\theta, t) = \int_{-\delta/2}^{\delta/2} \underbrace{\left\{ \sum_{j=1}^m \left[ \underbrace{W^j(\theta + \Delta\theta, t)}_{k_{cv}} i^j(t) \right] \right\}}_{k_{sv}} d(\Delta\theta) \quad (2)$$

$$= \sum_{v=1}^{\infty} F_v \cos(v\theta + \varphi_v)$$

where  $m$  is the phase number and  $\delta$  is the skewing angle.  $F_v$  is the  $v$ -th MMF harmonic amplitude, and  $\varphi_v$  is the corresponding phase angle. The relationship between  $F_v$  (or line-to-line flux linkage/EMF) and generic harmonic order  $v$  is

$$F_v \propto k_{sv} k_{cv} \frac{k_{wv}}{v} \quad (3)$$

To better understand the spatial-frequency-selection characteristic of winding, a comparison of all available 3-phase balanced winding for 12 slots is shown in Fig. 2, where spp means the slot number per pole per phase and the amplitude of MMF is calculated in p.u. with respect to the first MMF harmonic amplitude. The envelope is the absolute value of the well-known *sinc* function which is the continuous-time Fourier Transform of a symmetric periodic square wave in signal processing, showing the filtering nature of windings.

#### B. Modulation Operator

Mathematical operators, which reflect the mapping from primitive MMF distribution to eventual MMF distribution, are used to describe the modulation behaviors of different physical modulators. Here the primitive MMF distribution means the MMF distribution along the fictitious smooth cylindrical airgap peripheral, while the eventual MMF distribution means the actual airgap MMF distribution. The primitive MMF distribution  $f(\theta)$  is continuously differentiable and integrable, and  $f(\theta) = f(\theta + 2\pi)$ .

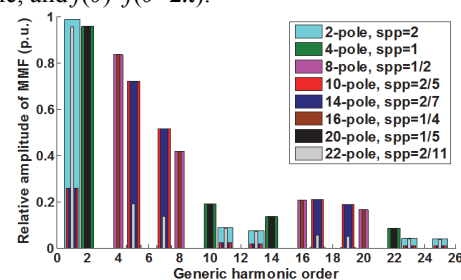


Fig. 2 Spectrums of available 3-phase 12-slot windings

#### 1) Short-circuited coils

In squirrel-cage IMs (SCIMs) and BDFIMs, the rotors are equipped with numbers of equally-spaced short-circuited coils to modify the time-variable primitive MMF distribution. The short-circuited coil is a passive device that relies on slip frequency between the primitive magnetizing MMF distribution (or primitive flux density distribution, usually a sinusoidally distributed one) and the modulator to induce current in the coil. At a given instant, the current flowing in  $j$ -th short-circuited coil establishes an extra magnetizing MMF as denoted by the dashed line in Fig. 3. As a result, the eventual

magnetizing MMF turns out to be the summation of primitive magnetizing MMF and all the extra ones established by the short-circuited coils, as shown in Fig. 3. The modulation behavior can be characterized by a modulation operator  $M(N_{SC}, \gamma)[\cdot]$  as

$$M(N_{SC}, \gamma)[f(\theta)] = f(\phi) + \sum_{j=1}^{N_{SC}} W^j i^j, \phi \in [0, 2\pi] \quad (4)$$

where  $N_{SC}$  is the number of short-circuited coil group, which reflects the switching state of the modulator per cycle.  $\gamma$  is the coil span factor of a specific coil, and  $i^j$  is the current flowing in the  $j$ -th coil.  $W^j$  is the winding function of the  $j$ -th coil.  $\phi$  is the angular position in the modulator-fixed reference frame, and  $\phi = \theta - \omega_r t$ .

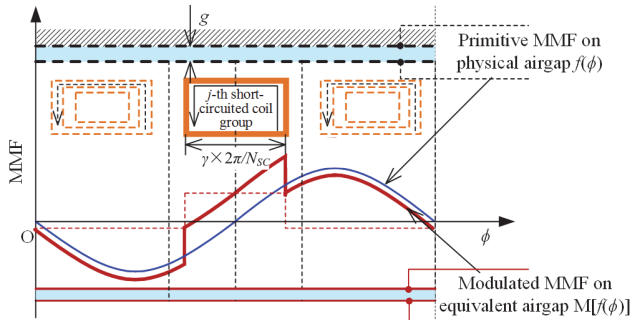


Fig. 3 The modulation principle of short-circuited coil

A typical BDFIM with  $p_f$ -pole-pair field winding,  $p_a$ -pole-pair armature winding, and  $N_{SC}$  single-layer short-circuited coil groups with the same coil span  $\gamma \times 2\pi / N_{SC}$  is taken as an example. When it is excited by a  $p_f$ -pole-pair unit cosine primitive magnetizing MMF, the eventual magnetizing MMF distribution contains harmonics whose pole pairs are  $p_f$  and  $lN_{SC} \pm p_f$ , where  $l$  is a positive integer. The relative amplitudes of each harmonic can be analytically determined and characterized by coefficients that are closely related to pole pair combination and coil span, which can be used to investigate the influence of pole pair combination and coil span on the performance, such as cross-coupling capability, torque density, etc. The detailed modulation process and spectrum shifting are shown in Fig. 4(a) and Fig. 4(b) respectively.

## 2) Variable Reluctance

The stator and rotor salient poles use alternative variation of magnetic reluctance to perform the modulation on an arbitrary primitive MMF distribution (even a uniform one), as shown in Fig. 5, and can be characterized by stator modulation operator  $M(N_{ST}, \varepsilon_{ST})[\cdot]$  and rotor modulation operator  $M(N_{RT}, \varepsilon_{RT})[\cdot]$ , where  $M(N_{ST}, \varepsilon_{ST})[\cdot]$  and  $M(N_{RT}, \varepsilon_{RT})[\cdot]$  are defined as mappings from an arbitrary function with a period of  $2\pi$  to a piecewise function on  $[0, 2\pi]$ ,

$$M(N_{ST}, \varepsilon_{ST})[f(\theta)] = \begin{cases} f(\phi), & \phi \in C^S, \\ \kappa(o_s / t_{ds}) f(\phi), & \phi \in [0, 2\pi] - C^S. \end{cases} \quad (5)$$

$$M(N_{RT}, \varepsilon_{RT})[f(\theta)] = \begin{cases} f(\phi), & \bar{\theta} \in C^R, \\ \kappa(o_r / t_{dr}) f(\phi), & \phi \in [0, 2\pi] - C^R. \end{cases} \quad (6)$$

where  $C^S$  and  $C^R$  are the discontinuous intervals occupied by stator and rotor teeth respectively in mechanical radians.  $N_{ST}$  and  $N_{RT}$  are numbers of stator and rotor teeth respectively.  $\kappa$  is the function of  $o/t_d$  to take into account the MMF drop over slot

opening [30], where  $o$  and  $t_d$  are the slot opening width and tooth pitch in radians. Subscription  $s$  and  $r$  denote the stator and rotor respectively. Large openings ( $o/t_d \geq 0.3$ ) are usually adopted in salient-pole rotors of SynRM, BDFRM, MGM and MG, stator pole for DCM, and both stator and rotor poles of stator-PM machines to perform field modulation. Under most circumstances the fine slotted stator/rotor ( $o/t_d < 0.3$ ) can be treated as a cylindrical one except those cases where the effects of small slotting is focused on, such as the study of harmonic losses in SCIM, cogging torque in PMSM, etc. The special case where there is no slotting or the slotting effect can be neglected is termed as unit modulation, which means no change is made on the primitive MMF distribution, and the corresponding modulator is unit.

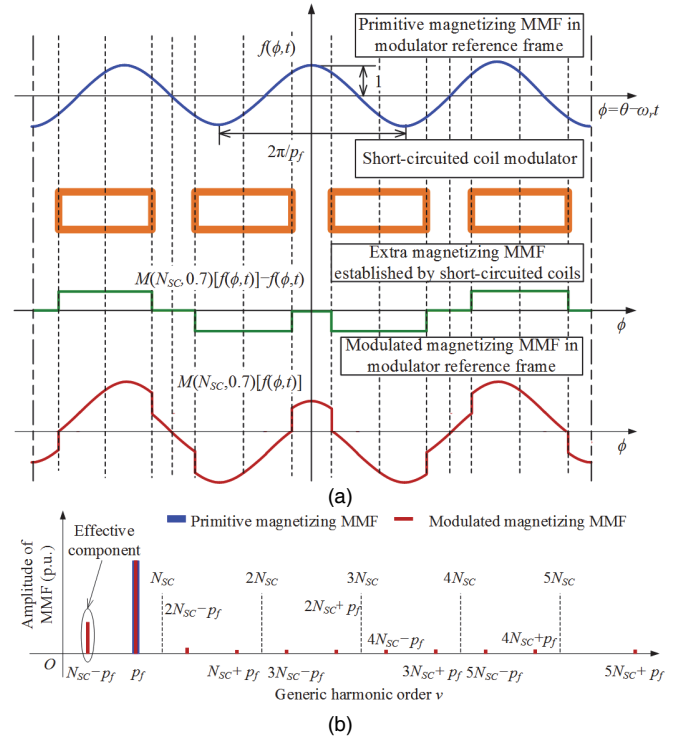


Fig. 4 The modulation of short-circuited coil modulator in a typical BDFIM ( $p_f=3$ ,  $p_a=1$ ,  $N_{SC}=4$ ). (a) Modulation process, (b) Spectrum shifting.

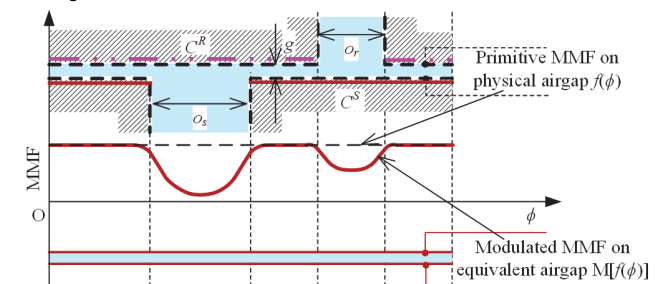


Fig. 5 The modulation principle of simple salient poles

Taking a typical BDFRM with a simple-salient-pole rotor as an example, The simple-salient-pole rotor modulator also produces harmonics with pole pair numbers of  $p_f$  and  $lN_{RT} \pm p_f$  in response to a  $p_f$ -pole-pair unit cosine primitive magnetizing MMF. The detailed modulation process of simple-salient-pole rotor modulator is shown in Fig. 6(a), and the corresponding spectrum shifting is shown in Fig. 6(b).

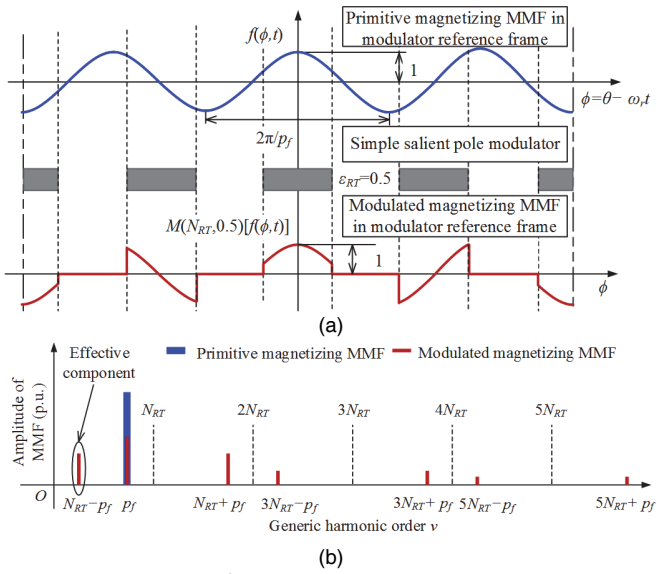


Fig. 6 The modulation of simple-salient-pole rotor modulator in a typical BDFRM ( $p=3$ ,  $p_a=1$ ,  $N_{RT}=4$ ). (a) Modulation process, (b) Spectrum shifting.

### 3) Flux guide

Flux guide modulates the non-uniform primitive MMF (i.e., the primitive MMF is not a constant dc value) by defining the path of flux lines, as shown in Fig. 7.

Flux guides are usually put together to form flux guide segment, sometimes also termed as flux barrier segment. Each flux guide segment consists of multiple layers magnetically insulated by non-magnetic materials. Therefore each layer behaves like a flux tube that only allows flux lines to enter or exit from the two points symmetrical around the middle line of each flux guide segment at  $(i+1/2)2\pi/N_{MB}$ . The MMF on the closed path through the two points will be equally shared by the airgaps at the two points if the airgap is assumed uniform which is usually the case. Then the flux guide can be characterized by an modulation operator  $M(N_{MB})[\cdot]$  as

$$M(N_{MB})[f(\phi)] = \frac{1}{2} \left[ f(\phi) - f\left( (2i+1) \frac{2\pi}{N_{MB}} - \phi \right) \right], \quad \phi \in \left( \frac{2\pi i}{N_{MB}}, \frac{2\pi(i+1)}{N_{MB}} \right) \quad (7)$$

where  $N_{MB}$  is the number of flux guide segment, which also reflects the switching state number of the modulator per cycle. Ideal flux guide is realized by axially-laminated anisotropic (ALA) structure. For ease of manufacture, multi-barrier structure is usually adopted.

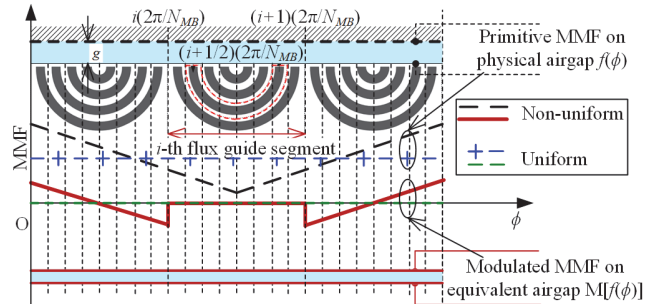


Fig. 7 The modulation principle of flux guide

Flux guide modulator is usually used in SynRM, BDFRM, FSPM machine, etc. Similar to the cases using short-circuited coil modulator and simple salient pole modulator, the modulation behavior performed by flux guide also produces three types of harmonics whose pole pairs are  $p_f$  and  $IN_{MB} \pm p_f$ . The detailed modulation process of flux guide modulator in a typical BDFRM with a multi-barrier rotor is shown in Fig. 8(a), and the corresponding spectrum shifting is shown in Fig. 8(b).

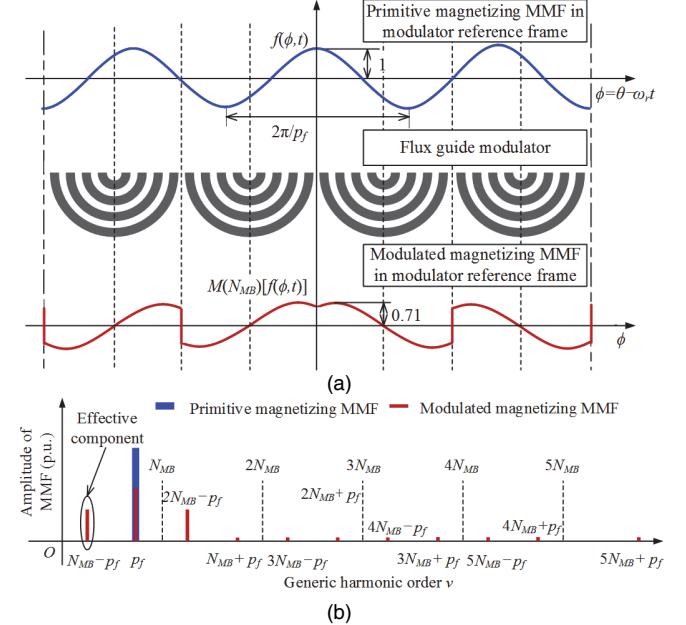


Fig. 8 The modulation of flux guide modulator in a typical BDFRM with a multi-barrier rotor ( $p=3$ ,  $p_a=1$ ,  $N_{MB}=4$ ). (a) Modulation process, (b) Spectrum shifting.

### 4) Property of modulation operator

All the modulations are manipulated in the modulator-fixed reference frame where the modulator is regarded as stationary to eliminate the effects of mechanical relative motion. For example, to analyze the FSPM, the stator modulator modulates the static magnetic field established by PMs, while the rotor modulator modulates the static magnetic field in rotor speed rotating coordinate system. As a mathematical operator, the modulation operator has some basic properties.

#### a) Linearity

The modulation operator is linear, that is,

$$M[\alpha f(\theta) + \beta g(\theta)] = \alpha M[f(\theta)] + \beta M[g(\theta)], \quad \alpha, \beta \in \mathbf{R} \quad (8)$$

#### b) Commutative law

The modulation operators satisfy the commutative law, that is,

$$M_1[M_2[f(\theta)]] = M_2[M_1[f(\theta)]] \quad (9)$$

#### c) Differential

The modulated primitive MMF is still differentiable.

#### d) Power

Arbitrary times of modulation by the same variable reluctance modulator or flux guide modulator is equivalent to a single modulation, but the short-circuited coil modulator is an exception.

$$\underbrace{M \left[ \dots M \left[ M \left[ f(\theta) \right] \right] \right]}_{k \text{ times}} = M \left[ f(\theta) \right] \quad (10)$$

### C. Modulation Factor

It is worth noting that though the airgap field modulation behavior shifts the location of the frequency domain spectral lines of the periodical primitive MMF, the total power content will not be changed no matter what kind of modulation is used. A field modulation factor (MF) can be defined as the ratio of the power of the effective MMF components of the eventual MMF distribution to that of the primitive MMF to describe the efficiency of modulation, i.e.,

$$\text{MF} = \sqrt{\frac{\sum_{\mu \in E} |F_{\mu}|^2}{\sum_{v=1}^{\infty} |F_v|^2}} = \sqrt{\frac{\sum_{\mu \in E} |F_{\mu}|^2}{\left\{ \frac{1}{2\pi} \int_{-\pi}^{\pi} [f(\theta)]^2 d\theta \right\}}} \quad (11)$$

where  $E$  is the set of orders of effective components of the modulated MMF. According to (11), the field modulation factors of single-layer short-circuited coil in Fig. 4, simple salient rotor pole in Fig. 6, multi-barrier rotor in Fig. 8 are 0.27, 0.318 and 0.318, respectively.

### D. Equivalent Airgap Model

By introducing the modulation operator, the physical airgap with windings, slots or flux guides nearby will be turned into an equivalent uniform one, as shown in Fig. 9, with the modulated MMF  $M[F_f(\theta, t)]$  and  $M[F_a(\theta, t)]$  expressed as

$$M[F_{f(a)}(\theta, t)] = M_n \left[ \dots M_2 \left[ M_1 \left[ F_{f(a)}(\theta, t) \right] \right] \right] \quad (12)$$

where  $F_f(\theta, t)$  is the primitive magnetizing MMF,  $F_a(\theta, t)$  is the primitive armature MMF, and

$$F_{f(a)}(\theta, t) = \sum_{j=1}^m [W_{f(a)}^j(\theta, t) \times i_{f(a)}^j(t)] \quad (13)$$

where  $W_f$  and  $W_a$  are the winding functions of the field winding and armature winding, respectively;  $i_f$  and  $i_a$  are magnetizing current and armature current respectively.

And the airgap flux density distribution can be obtained as

$$B_g(\theta, t) = \frac{\mu_0}{g} \{ M[F_f(\theta, t)] + M[F_a(\theta, t)] \} \quad (14)$$

where  $B_g$  is airgap flux density, and  $\mu_0$  is the vacuum permeability.

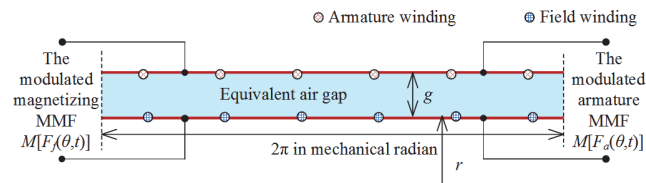


Fig 9 The equivalent airgap model

The no-load airgap flux density distribution is

$$B_f(\theta, t) = \frac{\mu_0}{g} M[F_f(\theta, t)] \quad (15)$$

The no-load flux linkage per phase linked by armature winding can be obtained as

$$\psi_a^j(t) = \mu_0 \frac{r_g L_{stk}}{g} \int M[F_f(\theta, t)] \times W_a^j(\theta, t) d\theta \quad (16)$$

where  $r_g$  is the radius of airgap,  $L_{stk}$  is the stack length.

The no-load EMF per phase in armature winding can be obtained by differentiating the flux linkage as

$$e_a^j(t) = -\frac{d}{dt} \left[ \mu_0 \frac{r_g L_{stk}}{g} \int M[F_f(\theta, t)] \times W_a^j(\theta, t) d\theta \right] \quad (17)$$

And the electromagnetic torque is

$$T_{em}(t) = -\frac{\mu_0 r_g^2 L_{stk}}{2g} \frac{\partial}{\partial \varphi} \int_0^{2\pi} \{ M[F_f(\theta, t)] + M[F_a(\theta, t)] \}^2 d\theta \quad (18)$$

### E. Signal Flow

The signal flow of an electrical machine is shown in Fig. 10. And it can be found that the performance of an electrical machine significantly depends on the combination of the three elements: source, modulator and filter.

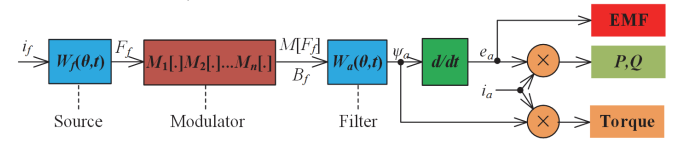


Fig. 10 The signal flow of an electrical machine

From the point of view of electromechanical energy conversion, at least one of the three elements has to move, and there will be in total  $(2^3-1)$  available combinations for a standard electrical machine with a single field winding, a single modulator and a single armature winding. It can be seen that the modulator can either be in synchronization with the primitive magnetizing (armature) MMF, which is termed as static (synchronous) modulation, or move relative to the primitive magnetizing (armature) MMF, which is termed as dynamic (asynchronous) modulation. In fact, the static modulation can be conceived as a special case of the dynamic modulation where the relative speed between the primitive magnetizing MMF and the modulator is zero. Behaviors of both modulations can be observed in conventional and newly-emerged electrical machines, and a general comparison between dynamic modulation and static modulation is given in TABLE I.

TABLE I  
COMPARISON BETWEEN DYNAMIC AND STATIC MODULATIONS

Modulation type	Dynamic (asynchronous) modulation	Static (synchronous) modulation
Relative speed between the primitive magnetizing MMF and the modulator	motion	rest
Field distribution	Irregular	Regular (sinusoidal or rectangular)
Number of effective spatial harmonic	Finite, at least two harmonics	Single or infinite (sinusoidal or rectangular field distribution)
Pole pair combination of field winding and armature winding	Close- or far-ratio match (larger EMF or larger torque)	Full match

## III. DEMONSTRATIONS

This Section shows the effectiveness and superiority of the general airgap field modulation theory in three typical applications, including but not limited to, topological analysis

of existing machine structures, analytical derivation of general design equations, and effective prediction of innovative machine topologies.

### A. Topological Analysis

Popular machine types in today's and previous comprehensive research are reviewed from the perspective of airgap field modulation mechanism, but only typical examples are presented here due to space limitation. In the following analysis,  $p_f$  and  $p_a$  denote the PPPN of field winding and armature winding, respectively;  $\omega_f$  and  $\omega_m$  denote the electrical angular frequency of primitive magnetizing MMF and mechanical rotor speed respectively. Plus and minus in front of pole pair number are used to distinguish the rotating direction of the field harmonics.

#### 1) DCM

The DCM is essentially an ac machine with a mechanical commutator. A typical DCM is shown in Fig. 11, together with the field modulation behavior.

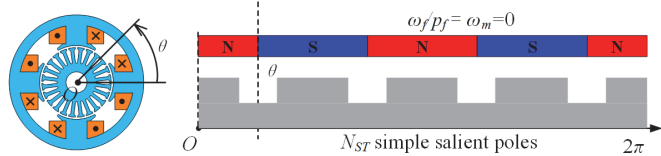


Fig. 11 DCM and the synchronous modulation behavior of salient stator poles

The stator usually adopts salient poles to wound the single-phase field winding which establishes a rectangular primitive magnetizing MMF on the airgap. The stator modulation operator characterizing the influence of stator poles on primitive magnetizing MMF distribution takes the form of (5), and static modulator occurs between the primitive magnetizing MMF and simple salient stator poles because no relative motion takes place between them. The modulated magnetizing MMF is then modulated by the rotor teeth asynchronously. Since the rotor is fine slotted, it makes negligible changes to the rectangular MMF distribution and can be treated as unit modulation under most circumstances.

The armature winding located on the rotor is a number of full-pitched or nearly full-pitched coils connected in series, which has a wide spectrum and allows all spatial harmonic components produced by the rectangular modulated magnetizing MMF to pass through, so triangular-wave flux linkage will be linked and rectangular EMF will be induced in each rotor coil.

#### 2) Salient-pole SM

The salient-pole wound-excitation SM which features a salient-pole rotor with pole shoes and dc field windings is shown in Fig. 12.

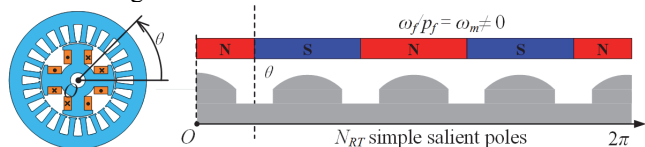


Fig. 12 Salient-pole SM and the synchronous modulation behavior of salient rotor poles

The dc field windings establish a rectangular primitive magnetizing MMF on the airgap which is then modulated synchronously by the salient rotor poles to produce a sinusoidal

magnetizing MMF distribution. The fine slotted stator also performs negligible asynchronous modulation to the sinusoidal MMF distribution. The armature winding located on the stator is preferred to be a multi-phase overlapping winding which only allows the spatial harmonic component of a certain PPPN to pass through. To maximize the flux linkage and EMF, the pole pair of the armature winding should be equal to that of the modulated magnetizing MMF.

### B. General Torque Density Equation

The electromagnetic torque produced by an electrical machine can be further derived into two typical forms from the unified formulation (18) according to the relative locations of field and armature windings. In most cases, the field winding and armature winding are placed on the stator and rotor separately (Type A), like in DCM and SM. Nevertheless, they can also be placed on the same stator or rotor (Type B), like in IM, SynRM, and most newly-emerged machines. The two torque producing types lead to distinct differences in torque calculation, so torque decomposition should be conducted first to analyze the torque production mechanism from the perspective of airgap field modulation.

#### 1) Torque decomposition

**Type A:** If the field winding and armature winding are placed on the separated stator and rotor, only the modulated magnetizing MMF depends on the position of rotor with respect to the same coordinate system, and (18) can be further expressed as

$$T_{emA}(t) = T_{Mff} + T_{Maf} \quad (19)$$

where

$$T_{Mff} = -\frac{\mu_0 r_g^2 L_{stk}}{g} \int_0^{2\pi} M[F_f(\theta, t)] d[F_f(\theta, t)] \quad (20)$$

$$T_{Maf} = -\frac{\mu_0 r_g^2 L_{stk}}{g} \int_0^{2\pi} M[F_a(\theta, t)] d[F_f(\theta, t)] \quad (21)$$

$T_{Mff}$  is solely produced by the interaction between the modulated magnetizing MMF and itself. A typical example of this torque component is the cogging torque in the PMSM, which contributes nothing to the average torque but causes periodic pulsation.  $T_{Maf}$  is produced by the interaction between the modulated magnetizing MMF and the modulated armature MMF, which accounts for the majority of electromagnetic torque.

**Type B:** If both the field winding and armature winding are placed on the same stator or rotor, both the modulated magnetizing and armature MMFs depend on the position of rotor with respect to the same coordinate system, and (18) can be further expressed as

$$T_{emB}(t) = T_{Mff} + T_{Maf} + T_{Mfa} + T_{Maa} \quad (22)$$

$$T_{Mfa} = -\frac{\mu_0 r_g^2 L_{stk}}{g} \int_0^{2\pi} M[F_f(\theta, t)] d[F_a(\theta, t)] \quad (23)$$

$$T_{Maa} = -\frac{\mu_0 r_g^2 L_{stk}}{g} \int_0^{2\pi} M[F_a(\theta, t)] d[F_a(\theta, t)] \quad (24)$$

Besides the two torque components  $T_{Mff}$  and  $T_{Maf}$  in Type A machine, another two torque components appear in Type B

machine.  $T_{Mfa}$  is produced by the interaction between the modulated armature MMF and the modulated magnetizing MMF.  $T_{Maa}$  depends on the interaction between modulated armature MMF and itself. Typical example of this torque component is the active torque in SRM, cogging torque in FSPM machine with the PMs removed and armature winding supplied.

Average torque decompositions of four typical machine topologies are given in Fig. 13. The torque proportion contributed by each field harmonic component is calculated with the method used in [31] based on airgap flux density radial and tangential components obtained from 2D finite element analysis (2D-FEA). It can be seen that, the torque of the 4-pole SCIM is dominated by the 2-pole-pair field harmonic. In 2/4 BDFIM and 4/2 BDFRM, the overall torques are primarily contributed by two field harmonics of dissimilar pole pairs, and the torque components are roughly proportional to the pole pairs. The total torque of the 12/10 FSPM machine is contributed by 6 dominating field harmonics. These six field harmonics forms 4 harmonic couples, that is, (6, 4), (6, 16), (18, -8) and (18, 28). Each harmonic couple can be conceptually conceived as a BDFRM.

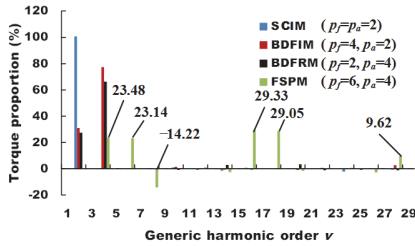


Fig. 13 Average torque decompositions of typical SCIM, BDFIM, BDFRM and FSPM

## 2) Torque density equation

Once the torque composition is determined, the effective average torque can be immediately obtained from the combination of (20), (21), (23) and (24). The unified expression of torque density for all electrical machines is not available because the expressions depend on not only the modulation type but also the relative location of field and armature windings. Here the general torque density equations for two typical machine types are derived to show the effectiveness of the methodology.

Based on (19), the general torque density equation for conventional machines, (SM, PMSM of Type A, IM and SynRM of Type B) in terms of rotor volume can be expressed as

$$TRV_A = \frac{\pi}{\sqrt{2}} \sum_v \overline{B_a^v} \overline{J_a^v} \cos \varphi_a^v \quad (25)$$

where  $\overline{B_a^v}$  and  $\overline{J_a^v}$  are the specific magnetic loading and specific electric loading of  $v$ -order harmonic of armature side respectively.

$$\overline{B_a^v} = 2B_{a(\text{amp})}^v / \pi \quad (26)$$

$$\overline{J_a^v} = 2m(N_a^j k_{wv}) I_{a(\text{rms})}^j / (\pi d) \quad (27)$$

where  $B_{a(\text{amp})}^v$  is the flux density amplitude of the  $v$ -order field

harmonic component.  $N_a^j$  is the number of turns in series of the  $j$ -th phase armature winding.  $I_{a(\text{rms})}^j$  is the rms value of the  $j$ -th phase armature current,  $d$  is the diameter of the airgap. The overall equivalent specific magnetic loading can be redefined as a kind of combination of  $v$ -order harmonic components.

Torque density equation for IM and SM which has already been widely used for initial sizing is just the special case of (25) by setting  $v=p_f$ , which means only the fundamental field harmonic is used for torque production.

Based on (22), the general torque density equation for some other typical type B machines (BDFRM, stator-PM machines) in terms of rotor volume is

$$TRV = \frac{\pi}{\sqrt{2}} \sum_v \frac{N_{RT(MB)}}{p_a^v} \overline{B_a^v} \overline{J_a^v} \cos \varphi_a^v \quad (28)$$

where  $p_a^v = N_{RT(MB)} \pm p_f^v$ ,  $p_f^v = (2k-1)p_f$ ,  $k \in \mathbf{Z}^+$ .

The FSPM machine is taken as an example. The primitive magnetizing MMF is established by single-phase concentrated winding containing static odd spatial harmonics, and the armature winding adopts fractional-slot concentrated winding, which possesses a wide spatial harmonic spectrum and can use heterodyned harmonics ( $N_{RT(MB)} \pm p_f^v$ ,  $N_{RT(MB)} \pm 3p_f^v$ , ...) to induce EMF and produce torque. The total torque is dominated by several field component pairs ( $p_a^v \pm p_f^v = N_{RT(MB)}$ ), and can be conceptually conceived as the superimposition of several BDFRMs. And for each working field harmonic pair, the torque produced by each pole pair is proportional to its pole pair number. For a typical 12/10 FSPM machine, the torque components produced by interaction between modulated magnetizing MMF and modulated armature MMF  $T_{p_f^v}$ , and those due to interaction between modulated armature MMF and modulated magnetizing MMF  $T_{N_{RT(MB)} \pm p_f^v}$  are linked by

$$T_{p_f^v} = \frac{p_f^v}{N_{RT(MB)} - p_f^v} T_{N_{RT(MB)} - p_f^v} - \frac{p_f^v}{N_{RT(MB)} + p_f^v} T_{N_{RT(MB)} + p_f^v} \quad (29)$$

The relationship (29) can be validated by the FEA results shown in Fig. 13. Torque density equations of other machines, like SRM and PMV of Type B can also be derived from (18) following similar torque decomposition and derivation procedure.

The estimated torque values based on (28) and radial flux density of each effective field harmonic component shown in Fig. 14(a) coincide well with the FEA (both 2D and 3D) and experimental results, as shown in Fig. 14(b). The 12/10 FSPM prototype is shown in Fig. 15 and its parameters are tabulated in TABLE II.

## C. Innovation in Machine Topology

Topological variations of stator-PM machines are taken as examples. As a typical stator-PM machines, the FSPM machine has become a very hot topic in both industrial and academic fields since its renaissance in 2005. FSPM machines are generally investigated by FEA [32], nonlinear magnetic circuit model [33], or subdomain model [34] (linear) for accurate calculation of airgap field distribution. Recently, attempts have



also been made to use simple MMF-permeance model in analysis of torque production mechanism [31], [35], but the application is rather limited, only confined to characterizing the generic harmonic orders and rotating speeds of airgap field components, and no relations between machine performance and topological structure has ever been developed.

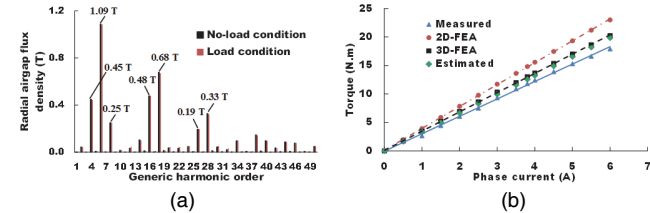


Fig. 14 FE-predicted and experimental results. (a) Spectrum of radial airgap flux density of conventional 12/10 FSPM machine (BLAC control mode with  $i_d=0$ ), (b) Electromagnetic torque with phase current rms value.

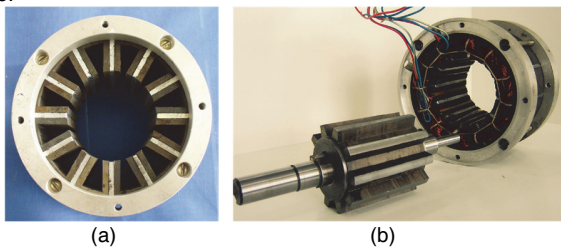


Fig. 15 FSPM prototype. (a) Stator, (b) Stator and rotor.

TABLE II  
PARAMETERS OF THE 12/10 FSPM PROTOTYPE

Item	Parameters
Stator outer, inner diameter (mm)	128, 70.4
Rotor inner diameter (mm)	22
Airgap length (mm)	0.35
Stack length (mm)	75
Turns in series per phase	280
Rotor tooth arc (degree)	10.5
PM, Silicon steel	N35SH, 50W470

Based on the proposed airgap field modulation theory, the working principle of the FSPM machine can be expressed as the ideal rectangular magnetizing MMF established by circumferentially placed PM array is first synchronously modulated by the simple salient stator poles and later asynchronously modulated by the simple salient rotor poles, whose behaviors are considered as the stator modulation operator and rotor modulation operator. The modulated MMF exerted on the virtual uniform airgap produces the necessary field distribution. The concentrated winding wound around the stator teeth extracts the active field components to produce induced EMF, and electromagnetic torque is produced when a current synchronous to the EMF is forced into the stator winding.

Topologically, the machines are only relevant with the primitive magnetizing MMF, two modulation operators and the armature winding, and do not care about the specific location and form of the three elements.

#### 1) Changes in primitive magnetizing MMF

If the PM array is moved from the tooth interior in conventional FSPM machine [36] to stator yoke [37], a feasible variable reluctance permanent magnet (VRPM) machine is produced, as shown in Fig. 16.

The switching process includes 3 steps, as shown in Fig. 17.

Step 1: The PM array is rotated around the origin clockwise by half tooth pitch ( $\pi/12$  in radians) logically.

Step 2: Each U-core is split into two to accommodate PM arrays, and every two adjacent half U-cores are merged to form a T-core.

Step 3: The radial length of PM array is shortened to fit the yoke height.

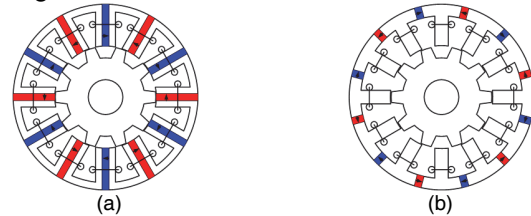


Fig. 16 Variants of the FSPM machine due to changes in primitive magnetizing MMF. (a) Conventional 12/10 FSPM [36], (b) VRPM with PM in the yoke [37].

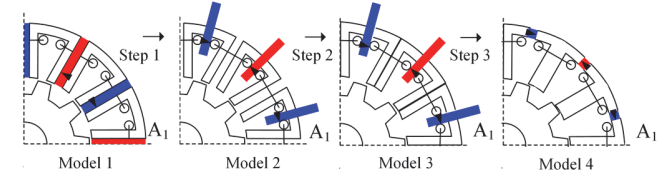


Fig. 17 The switching process from conventional 12/10 FSPM to 12/10 VRPM with PM in the yoke

2D-FEA predicted no-load EMFs of the conventional 12/10 FSPM machine (Model 1) and the VRPM machine (Model 4) are shown in Fig. 18, together with the experimentally measured no-load EMF at 1200 r/min. The per-phase EMFs of VRPM are scaled up 5.26 times (the overall volume consumed by the FSPM is 5.26 times that of the VRPM) so as to have comparable amplitudes with those of the FSPM for clarity. It can be observed that the per-phase EMF of 12/10 FSPM is almost ideally sinusoidal. In contrast, a significant 5-th harmonic component appears in EMF of the VRPM, and phase difference between the two EMFs is about  $\pi/4$ .

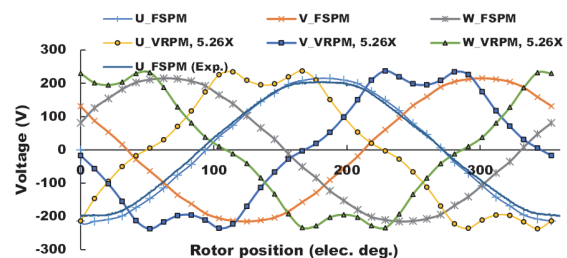


Fig. 18 No-load EMFs of Model 1 and Model 4 (1200 r/min)

#### 2) Changes in modulator

If the stator and rotor modulation operators are modified rather than the primitive MMF source, a breed of variants of conventional FSPM is obtained, as shown in Fig. 19.

#### 3) Changes in armature winding

If the armature winding is changed solely, a variant branch is obtained, as shown in Fig. 20.

#### 4) Changes in relative location

If the stator or rotor is partitioned and the relative location of the three elements are changed, the partitioned stator FSPM machine and magnetically-gear dual-rotor motor can also be obtained, as shown in Fig. 21.

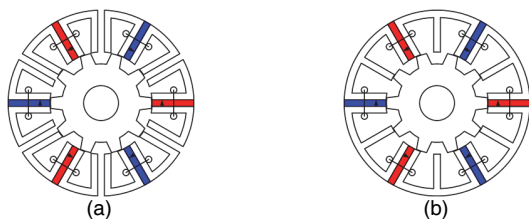


Fig. 19 Variants of the FSPM machine due to changes in modulator. (a) Type A2 [36], (b) E-core FSPM [38].

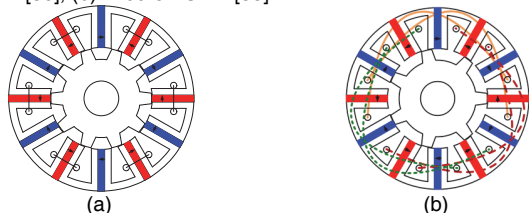


Fig. 20 Variants of the FSPM machine due to changes in armature winding. (a) Alternate pole wound FSPM [39], (b) Distributed winding FSPM [40].

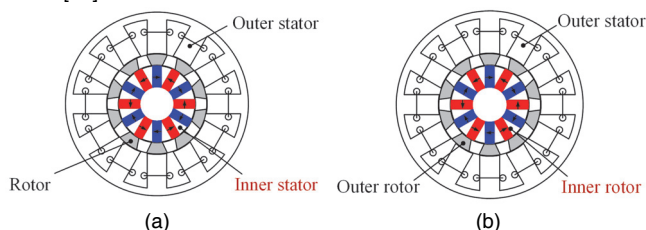


Fig. 21 Variants of the FSPM machine due to changes in relative location. (a) Partitioned-stator FSPM [41], (b) Magnetically-g geared dual-rotor motor [42].

#### IV. CONCLUSION

This paper theorizes a rather generalized airgap field modulation phenomenon of electrical machines by introducing the analogy between the electrical machine and the switching converter for the first time, which indicates that the performance of an electrical machine depends heavily on the cascade of three elementary parts, that is, the primitive magnetizing MMF, the modulator and the armature winding. All the conventional machines, including DCM, IM, and SM, comply with the field modulation theory and can be considered as special cases of the general field modulated machines.

The primitive magnetizing MMF and the armature winding can be analyzed and designed by the frequency-selection feature of windings characterized by winding factor, composition factor and skew factor. The modulator is characterized by the modulation operator, which defines the mapping from primitive MMF distribution function to eventual MMF distribution function.

Based on the proposed general field modulation theory, all electrical machines with magnetically anisotropic stator and rotor can be equivalent to a cylindrical one with an equivalent smooth airgap. General equations for no-load and loaded airgap field distributions, no-load flux linkage linked by armature winding, no-load EMF, and electromagnetic torque are derived. Two basic machine types are identified by the torque composition, and two distinct modulation types, namely, synchronous and asynchronous modulations are found and compared in detail.

The superiority of the developed general airgap field modulation theory over existing ones can be summarized as:

1) It is valid for all electromagnetic machines, irrespective of DC or AC machines, salient or non-salient machines, sinusoidal or rectangular driving machines, etc.

2) It can perform not only the qualitative analysis with clear physical meaning, but also quantitative analysis of electrical machines.

3) It can not only analyze the available electric machines, but also guide the invention of new machine topologies.

More analysis and applications of the proposed general field modulation theory to other types of machines will be reported in separate papers in near future.

#### REFERENCES

- [1] S. Sul, "Introduction," in *Control of electric machine drive systems*, 1<sup>st</sup> ed. New York: John Wiley & Sons, 2011, pp. 1-35.
- [2] M. E. Talaat, "Steady-state and transient synthesis of 3-phase reluctance motors (synchronous motors without field excitation)," *Trans. AIEE*, vol. 70, DOI: 10.1109/T-AIEE.1951.5060658, no. 2, pp. 1963-1970, Jul. 1951.
- [3] M. W. Brainard, "Synchronous machines with rotating permanent-magnet fields Part I. Characteristics and Mechanical Construction," *Trans. AIEE. Part III: Power Apparatus and Syst.*, vol. 71, DOI: 10.1109/AIEEPAS.1952.4498525, no. 1, pp. 670-676, Jan. 1952.
- [4] K. T. Chau, C. C. Chan, and C. Liu, "Overview of permanent-magnet brushless drives for electric and hybrid electric vehicles," *IEEE Trans. Ind. Electron.*, vol. 55, DOI: 10.1109/TIE.2008.918403, no. 6, pp. 2246-2257, Jun. 2008.
- [5] C. H. Lee, "Vernier motor and its design," *IEEE Trans. Power Apparatus Syst.*, vol. 82, DOI: 10.1109/TPAS.1963.291362, no. 66, pp. 343-349, Jun. 1963.
- [6] A. R. W. Broadway, L. Burbridge, "Self-cascaded machine: a low speed motor or high frequency brushless alternator," *Proc. IEE*, vol. 117, DOI: 10.1049/piee.1970.0247, no. 7, pp. 1277-1290, Jul. 1970.
- [7] P. Han, M. Cheng, and R. Luo, "Design and analysis of a brushless doubly-fed induction machine with dual-stator structure," *IEEE Trans. Energy Convers.*, vol. 31, DOI: 10.1109/TEC.2016.2547955, no. 3, pp. 1132-1141, Sep. 2016.
- [8] A. R. W. Broadway, "Cageless induction machine," *Proc. IEE*, vol. 118, DOI: 10.1049/piee.1971.0290, no. 11, pp. 1593-1600, Nov. 1971.
- [9] E. R. Laithwaite, J. F. Eastham, H. R. Bolton, and T. G. Fellows, "Linear motors with transverse flux," *Proc. IEE*, vol. 118, DOI: 10.1049/piee.1971.0328, no. 12, pp. 1761-1767, Dec. 1971.
- [10] P. J. Lawrenson, J. M. Stephenson, P. T. Blenkinsop, J. Corda, and N. N. Fulton, "Variable-speed switched reluctance motors," *IEE Proc. -Electr. Power Appl.*, vol. 127, DOI: 10.1049/ip-b:19800034, no. 4, pp. 253-265, Jul. 1980.
- [11] Y. Liao, F. Liang, and T. A. Lipo, "A novel permanent magnet motor with doubly salient structure," in *Conf. Rec. IEEE IAS Annu. Meeting*, vol. 1, DOI: 10.1109/IAS.1992.244279, pp. 308-314, Oct. 1992.
- [12] M. Cheng, W. Hua, J. Zhang, and W. Zhao, "Overview of stator-permanent magnet brushless machines," *IEEE Trans. Ind. Electron.*, vol. 58, DOI: 10.1109/TIE.2011.2123853, no. 11, pp. 5087-5101, Nov. 2011.
- [13] A. Toba, T. A. Lipo, "Novel dual-excitation permanent magnet vernier machine," in *Conf. Record of IEEE IAS Annu. Meeting*, vol. 4, DOI: 10.1109/IAS.1999.799197, pp. 2539-2544, Oct. 1999.
- [14] K. Atallah, S. D. Calverley, and D. Howe, "Design, analysis and realisation of a high-performance magnetic gear," *IEE Proc. - Electr. Power Appl.*, vol. 151, DOI: 10.1049/ip-epa:20040224, no. 2, pp. 135-143, Mar. 2004.
- [15] K. Atallah, J. Rens, S. Mezani, and D. Howe, "A novel 'pseudo' direct-drive brushless permanent magnet machine," *IEEE Trans. Magn.*, vol. 44, DOI: 10.1109/TMAG.2008.2001509, no. 12, pp. 4605-4617, Dec. 2008.
- [16] K. T. Chau, D. Zhang, J. Z. Jiang, C. Liu, and Y. Zhang, "Design of a magnetic-g geared outer-rotor permanent-magnet brushless motor for electric vehicles," *IEEE Trans. Magn.*, vol. 43, DOI: 10.1109/TMAG.2007.893714, no. 6, pp. 2504-2506, Jun. 2007.
- [17] Y. Fan, L. Zhang, M. Cheng, and K. T. Chau, "Sensorless SVPWM-FADTC of a new flux-modulated permanent-magnet wheel motor based on a wide-speed sliding mode observer," *IEEE Trans. Ind.*

IEEE TRANSACTIONS ON INDUSTRIAL ELECTRONICS

*Electron.*, vol. 62, DOI: 10.1109/TIE.2014.2376879, no. 5, pp. 3143-3151, May 2015.

[18] X. Sun, M. Cheng, W. Hua, and L. Xu, "Optimal design of double-layer permanent magnet dual mechanical port machine for wind power application," *IEEE Trans. Magn.*, vol. 45, DOI: 10.1109/TMAG.2009.2021526, no. 10, pp. 4613-4616, Sep. 2009.

[19] T. A. Lipo, "Winding distribution in an ideal machine," in *Analysis of synchronous machine*, 2<sup>nd</sup> ed., CRC Press, 2012, pp. 1-76.

[20] D. A. Staton, W. L. Soong, R. P. Deodhar, and T. J. E. Miller, "Unified theory of torque production in ac, dc and reluctance motors," in *Conf. Rec. IEEE IAS Annu. Meeting*, vol. 1, DOI: 10.1109/IAS.1994.345485, pp. 149-156, Oct. 1994.

[21] K. L. Hansen, "The rotating magnetic field theory of A-C motors," *Journal of AIEE*, vol. 44, DOI: 10.1109/JAIEE.1925.6536172, no. 2, pp. 170-178, Feb. 1925.

[22] H. R. West, "The cross-field theory of alternating-current machines," *Trans. AIEE*, vol. XLV, DOI: 10.1109/T-AIEE.1926.5061238, pp. 466-474, Jan. 1926.

[23] R. E. Doherty, C. A. Nickle, "Synchronous machines I – an extension of Blondel's two-reaction theory," *Trans. AIEE*, vol. XLV, DOI: 10.1109/T-AIEE.1926.5061289, pp. 912-947, Jan. 1926.

[24] R. K. Park, "Two-reaction theory of synchronous machine generalized method of analysis – Part I," *Trans. AIEE*, vol. 48, DOI: 10.1109/T-AIEE.1929.5055275, no. 3, pp. 716-727, Mar. 1929.

[25] B. Adkins, R. G. Harley, *The General Theory of Alternating Current Machines*. London: Chapman and Hall Ltd., 1975.

[26] J. Fienne, "New approach to general theory of electrical machines using magnetic equivalent circuit," *Proc. IEE*, vol. 120, DOI: 10.1049/piee.1973.0018, no. 1, pp. 94-104, Jan. 1973.

[27] C. E. Linkous, "Effect of skew on induction motor magnetic fields," *Trans. AIEE. Part III: Power Apparatus and Syst.*, vol. 74, DOI: 10.1109/AIEEPAS.1955.4499143, no. 3, pp. 760-765, Jan. 1955.

[28] T. Ishikawa, G. R. Slemon, "A method of reducing ripple torque in permanent magnet motors without skewing," *IEEE Trans. Magn.*, vol. 29, DOI: 10.1109/20.250808, no. 2, pp. 2028-2031, Mar. 1993.

[29] R. P. Deodhar, D. A. Staton, and T. J. E. Miller, "Modeling of skew using the flux-mmF diagram," *IEEE Trans. Ind. Appl.*, vol. 32, DOI: 10.1109/28.556637, no. 6, pp. 1339-1347, Nov./Dec. 1996.

[30] B. Heller, V. Hamata, *Harmonic Field Effects in Induction Machines*. Amsterdam, The Netherlands: Elsevier, 1977.

[31] Z. Z. Wu, Z. Q. Zhu, "Analysis of air-gap field modulation and magnetic gearing effects in switched flux permanent magnet machines," *IEEE Trans. Magn.*, vol. 51, DOI: 10.1109/TMAG.2015.2402201, no. 5, May. 2015, Article #: 8105012.

[32] J. T. Chen, Z. Q. Zhu, S. Iwasaki and R. P. Deodhar, "Influence of slot opening on optimal stator and rotor pole combination and electromagnetics performance of switched-flux PM brushless ac machines," *IEEE Trans. Ind. Appl.*, vol. 47, DOI: 10.1109/TIA.2011.2155011, no. 4, pp. 1681-1691, Jul./Aug. 2011.

[33] J. T. Chen, Z. Q. Zhu, "Influence of the rotor pole number on optimal parameters in flux-switching PM brushless ac machines by the lumped-parameter magnetic circuit model," *IEEE Trans. Ind. Appl.*, vol. 46, DOI: 10.1109/TIA.2010.2049720, no. 4, pp. 1381-1388, Jul./Aug. 2010.

[34] K. Boughrara, T. Lubin and R. Ibtouen, "General subdomain model for predicting magnetic field in internal and external rotor multiphase flux-switching machines topologies," *IEEE Trans. Magn.*, vol. 49, DOI: 10.1109/TMAG.2013.2260827, no. 10, pp. 5310-5325, Oct. 2013.

[35] J. D. McFarland, T. M. Johns, A. M. EL-Refaei, "Analysis of the torque production mechanism for flux-switching permanent-magnet machines," *IEEE Trans. Ind. Appl.*, vol. 51, DOI: 10.1109/TIA.2015.2411655, no. 4, pp. 3041-3049, Jul./Aug. 2015.

[36] E. Hoang, A. H. Ben-Ahmed, and J. Lucidarme, "Switching flux permanent magnet polyphased synchronous machines," in *Proc. Eur. Conf. Power Electron. Appl.*, HAL ID: hal-00533004, pp. 903-908, Sep. 1997.

[37] D. Wu, J. T. Shi, Z. Q. Zhu, and X. Liu, "Electromagnetic performance of novel synchronous machines with permanent magnets in stator yoke," *IEEE Trans. Magn.*, vol. 50, DOI: 10.1109/TMAG.2014.2317794, no. 9, Sep. 2014, Article#: 8102009.

[38] J. T. Chen, Z. Q. Zhu, S. Iwasaki and R. P. Deodhar, "A novel E-core switched-flux PM brushless ac machine," *IEEE Trans. Ind. Appl.*, vol. 47, DOI: 10.1109/TIA.2011.2126543, no. 3, pp. 1273-1282, May/June, 2011.

[39] R. L. Owen, Z. Q. Zhu, A. S. Thomas, G. W. Jewell, and D. Howe, "Alternate poles wound flux-switching permanent magnet brushless ac machines," *IEEE Trans. Ind. Appl.*, vol. 46, DOI: 10.1109/TIA.2009.2039913, no. 2, pp. 790-797, Mar/Apr, 2010.

[40] Y. Du, F. Xiao, W. Hua, X. Zhu, M. Cheng, L. Quan, et al. "Comparison of flux-switching PM motors with different winding configurations using magnetic gearing principle," *IEEE Tans. Magn.*, vol. 52, DOI: 10.1109/TMAG.2015.2513742, no. 5, May 2016. Article #: 8201908.

[41] Z. Q. Zhu, D. Evans, "Overview of recent advances in innovative electrical machines – with particular reference to magnetically geared switched flux machines," in *Proc. Int. Conf. Electr. Mach. Syst. (ICEMS)*, DOI: 10.1109/ICEMS.2014.7013921, pp.1-10, Oct. 2014.

[42] L. Sun, M. Cheng, H. Jia, "Analysis of a novel magnetic-geared dual-rotor motor with complementary structure," *IEEE Trans. Ind. Electron.*, vol. 62, DOI: 10.1109/TIE.2015.2437361, no. 11, pp. 6737-6747, Nov. 2015.



**Ming Cheng** (M'01–SM'02–F'15) received the B.Sc. and M.Sc. degrees in Electrical Engineering from the Department of Electrical Engineering, Southeast University, Nanjing, China, in 1982 and 1987, respectively, and the Ph.D. degree from the Department of Electrical and Electronic Engineering, The University of Hong Kong, Hong Kong, in 2001.

Since 1987, he has been with Southeast University, where he is currently a Distinguished Professor in the School of Electrical Engineering and the Director of the Research Center for Wind Power Generation. From January to April 2011, he was a Visiting Professor with the Wisconsin Electric Machine and Power Electronics Consortium, University of Wisconsin-Madison. His teaching and research interests include electrical machines, motor drives for electric vehicles, and renewable energy generation. He has authored or coauthored over 350 technical papers and 4 books and is the holder of 90 patents in these areas.

Prof. Cheng is a fellow of the Institution of Engineering and Technology. He has served as chair and organizing committee member for many international conferences. He is a Distinguished Lecturer of the IEEE Industry Applications Society (IAS) in 2015/2016.



**Peng Han** (S'12) received the B.S. degree in electrical engineering from Southeast University, Nanjing, China, in 2012, where he is currently working towards the Ph.D. degree in the School of Electrical Engineering.

From November 2014 to November 2015, he was a joint Ph.D. student funded by China Scholarship Council with the Department of Energy Technology, Aalborg University, Aalborg, Denmark, where he focused on the brushless doubly-fed machines for wind energy conversion and high power drive. His current research interests include design, analysis, and control of brushless doubly-fed machines.



**Wei Hua** (M'03–SM'16) received B.Sc. and Ph.D. degrees in Electrical Engineering from Southeast University, Nanjing, China, in 2001 and 2007, respectively.

Since 2007, he has been with Southeast University, where he is currently a Professor with the School of Electrical Engineering. He is the author or coauthor of over 140 technical papers, and he is the holder of 30 patents in his areas of interest. His teaching and research interests include the design, analysis, and control of electrical machines.